AD-A072 204 NAVY UNDERWATER SOUND LAB NEW LONDON CT F/G 17/1

EFFECTS OF BEAM STEERING ON THE BEHAVIOR OF PLANAR ARRAYS.(U)

MAR 66 D T PORTER

UNCLASSIFIED USL-TM-960-28-66 NL

1 OF 1

AD

A072204

END

DATE

FILMED

9 79

DDC

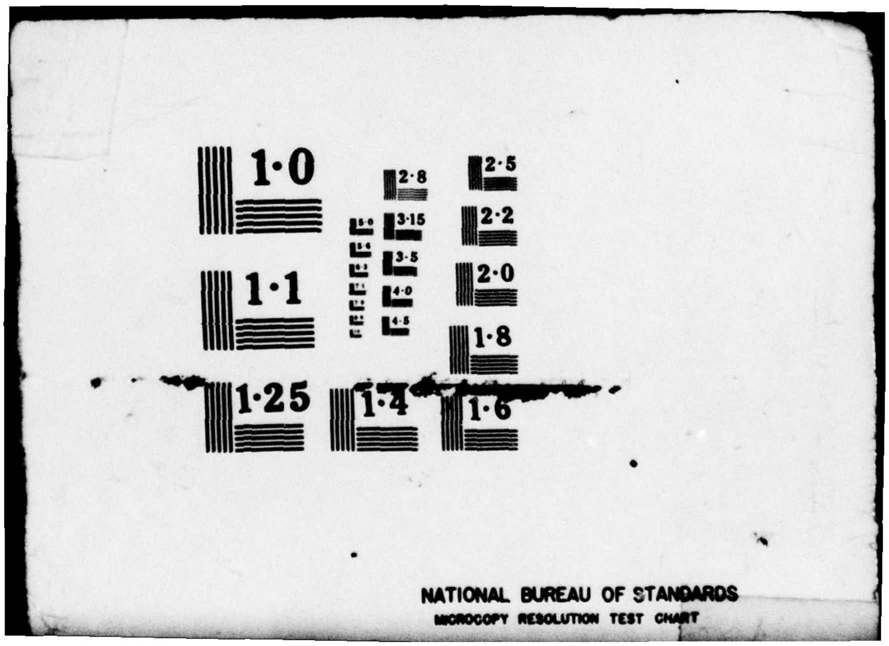
1·0
2·8
2·5
3·15
2·2
3·5
2·0
4·0
1·1
4·5
1·8
1·25
1·4
1·6
NATIONAL BUREAU OF STANDARDS
MICROCOPY RESOLUTION TEST CHART

UNCLASSIFIED

Copy No. 24

USL Tech Memo
6-1-452-00-00
SF101 03 18-11213

U. S. Navy Underwater Sound Laboratory
Fort Trumbull, New London, Connecticut

EFFECTS OF BEAM STEERING ON THE BEHAVIOR OF PLANAR ARRAYS

By

David T. Porter

USL Technical Memorandum No. 960-28-66

28 March 1966

This memorandum is a continuation of reference ~~(a)~~, which discussed the effects of the transducer internal impedance (Z^I, or Z_{oc}) upon the behavior of unsteered planar arrays. A detailed discussion of the effects of the components of the transducer equivalent circuit upon Z^I is contained in another reference ~~(b)~~. Results are presented in this memorandum showing the effects of beam steering and Z^I upon the behavior of 80 element planar arrays. Three main criteria will be used in evaluating the behavior of the arrays: cavitation-limited power, velocity-limited power, and the occurrence of negative radiation resistances.

ARRAYS CONSIDERED

The arrays were all 8 rows by 10 columns, as shown in figure 1.

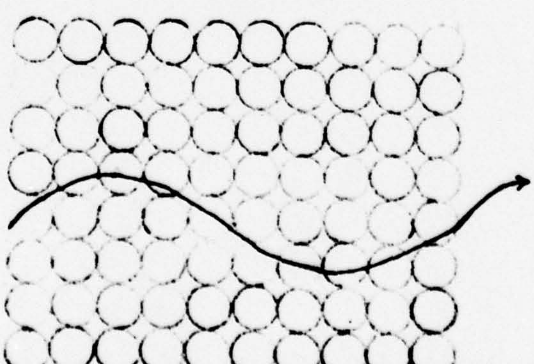

Figure 1 A Steered Array of 80 Elements

UNCLASSIFIED

UNCLASSIFIED

SECURITY CLASSIFICATION OF THIS PAGE (When Data Entered)

REPORT DOCUMENTATION PAGE

READ INSTRUCTIONS BEFORE COMPLETING FORM

1. REPORT NUMBER	2. GOVT ACCESSION NO. 960-28-66	3. RECIPIENT'S CATALOG NUMBER
4. TITLE (and Subtitle) EFFECTS OF BEAM STEERING ON THE BEHAVIOR OF PLANAR ARRYAS		5. TYPE OF REPORT & PERIOD COVERED Tech Memo
		6. PERFORMING ORG. REPORT NUMBER
7. AUTHOR(s) Porter, David T.		8. CONTRACT OR GRANT NUMBER(s) Nonr-266(84)
9. PERFORMING ORGANIZATION NAME AND ADDRESS Naval Underwater Systems Center New London, CT		10. PROGRAM ELEMENT, PROJECT, TASK AREA & WORK UNIT NUMBERS
11. CONTROLLING OFFICE NAME AND ADDRESS Office of Naval Research, Code 220 800 North Quincy St. Arlington, VA 22217		12. REPORT DATE 28 MAR 66
		13. NUMBER OF PAGES
14. MONITORING AGENCY NAME & ADDRESS (if different from Controlling Office)		15. SECURITY CLASS. (of this report) UNCLASSIFIED
		15a. DECLASSIFICATION/DOWNGRADING SCHEDULE

16. DISTRIBUTION STATEMENT (of this Report)

Approved for public release; distribution unlimited.

17. DISTRIBUTION STATEMENT (of the abstract entered in Block 20, if different from Report)

18. SUPPLEMENTARY NOTES

19. KEY WORDS (Continue on reverse side if necessary and identify by block number)

20. ABSTRACT (Continue on reverse side if necessary and identify by block number)

DD FORM 1 JAN 73 1473 EDITION OF 1 NOV 65 IS OBSOLETE

S/N 0102-LF-014-6601

UNCLASSIFIED

SECURITY CLASSIFICATION OF THIS PAGE (When Data Entered)

They were composed of identical close-packed circular pistons in an infinite rigid baffle. Three values of the piston ka were used: 0.5 ($\lambda/6$ approximate diameter), 1.0 ($\lambda/3$ approximate diameter) and 1.5 ($\lambda/2$ approximate diameter). The resistive part of Z^I,R^I, was taken to be zero, but seven different values of the reactive part of Z^I,X^I, were used. The values of X^I are given in terms of the ratio X^I/X_{11}, where X_{11} is the self radiation reactance of the piston alone in the baffle. The ratio X^I/X_{11} was taken as +1, 0, -1, -2, -3, -5, and ∞. For the jth element of an array, the Thevenin equivalent driving force (G_j), the velocity (V_j), the radiation impedance (Z_{rj}), and Z^I are related by

$$G_j = V_j(Z_{rj}+Z^I). \tag{1}$$

The driving forces were all taken equal, so that an X^I of ∞ caused equal velocity magnitudes. The arrays were steered in the direction of the longer side of the array, by keeping a constant phase difference between the driving forces in adjacent columns. Due to the mutual coupling, the velocity phases do not necessarily maintain this phase difference, so that the maximum response of the transmitted beam is not necessarily at the desired steering angle. Figure 2 shows a portion of the pattern for the case of $X^I/X_{11}=-1$, ka=1.0, and θ_{st} (steering angle away from broadside)=60°. The computer results from which figure 2 was taken show that the maximum response occurs at about θ=57°, but the response at the desired steering angle is only 0.1 db down from the maximum.

CAVITATION-LIMITED POWER

Figures 3a, 3b, and 3c show the effect of steering on cavitation-limited power. With a few minor exceptions, cavitation-limited power steadily decreases as the steering angle increases. The cavitation-limited powers are normalized to the cavitation-limitation power for the unsteered case with equal velocities. As shown in reference (a) for the unsteered case, cavitation-limited power is higher for the cases with Z^I=0 than for the equal velocity cases. Table I gives a summary of the advantages in cavitation-limited power of Z^I=0 over the equal velocity cases.

Table I

Advantage in Cavitation-Limited Power (Db)
of $Z^I=0$ over Equal Velocities

ka	$\theta_{st}=0^\circ$(Broadside)	$\theta_{st}=90^\circ$(Endfire)
0.5	2.2	4.1
1.0	2.1	3.9
1.5	1.6	2.4

As is shown in Appendix B of reference (a), the peak pressure on a piston is closely related to the acoustic force on the piston. The acoustic force is obtained from

$$\text{Acoustic Force} = (\text{Radiation Impedance})\times(\text{Velocity}) \qquad (2)$$

Equations (1) and (2) show that when $Z^I=0$, the driving forces become equal to the acoustic forces. When the acoustic forces are equal, the pressure distribution on the array becomes nearly uniform, as is shown in figure 6b of reference (a). However, for the equal-velocity case, the acoustic forces are directly proportional to the radiation impedances, which vary considerably over the array, and will vary to a greater extent for larger steering angles. The cavitation-limited power for all values of Z^I also decreases as θ_{st} increases because the acoustic load on the pistons becomes more and more reactive as θ_{st} increases. Table II gives the average radiation resistances ($R/\rho cA$) that were computed, and Table III gives the average radiation reactances ($X/\rho cA$). Note that the average radiation reactance increases much more rapidly than the resistance as θ_{st} increases.

The cavitation-limited power index γ was presented in reference (c) by Sherman. In reference (d), Chin computed γ for some rectangular radiators with traveling waves imposed on them in such a way as to simulate steered arrays of small close-packed pistons (with velocities equal). As would be expected, Chin's graphs of γ versus θ_{st} have the same shape as the graphs given here in figures 3a, 3b, and 3c.

VELOCITY-LIMITED POWER

Figures 4a, 4b, and 4c show the effects of steering on velocity-limited power. Straight line segments were used to connect the discrete points for which the computations were done. As would be expected, the equal-velocity cases ($X^I=\infty$) have the greatest velocity-limited power, as all of their pistons are at the maximum permissable velocity. The powers in figures 4a, 4b, and 4c are again normalized to the equal-velocity, unsteered cases. The $Z^I=0$ cases have much less velocity-limited power than the equal-velocity cases, as the $Z^I=0$ cases force their pistons to maintain a constant product of velocity and radiation impedance, so that many pistons will be operating far below the permissable limit. As θ_{st} increases, the variation in radiation impedances grows worse, so that the upstream end of the array has high velocities and low radiation impedances, and the downstream end of the array has low velocities and high radiation impedances, and neither end is able to radiate a large amount of acoustic power.

For the cases where X^I/X_{11} was -1 or -2, poor velocity control was usually present, so that velocity-limited power was low. For these cases, velocity-limited power generally continued to decrease as θ_{st} increased. However, for the equal velocity cases and the other cases where velocity control was generally good (X^I/X_{11}=+1, -3, and -5), velocity-limited power reached a maximum for some sizeable steering angle. These "optimum" steering angles appeared to be near 45° for ka=0.5, 60° for ka=1.0, and 75° for ka=1.5. However, this optimum steering angle is mainly determined by the size of the array, not the size of the pistons in it. In reference (d), Chin also gave results for the radiation resistance for the rectangular radiator model of a steered array. When the velocity level is fixed, the radiation resistance then determines the acoustic power. Therefore, Chin's results for the radiation resistance of the steered rectangle are closely related to the velocity-limited power of a close-packed array of the same outer dimensions as the rectangle. Unfortunately, Chin did not have a rectangle of the same outer dimensions as the 80 element array in this report. However, his figures 5 and 6 do show rectangles with maximum radiation resistances at large steering angles.

OCCURRENCE OF NEGATIVE RADIATION RESISTANCES

Table IV gives the number of elements having negative radiation resistances in each of the arrays considered. Elements having negative radiation resistances are absorbing power from the rest of the array, and are evidence of badly behaved arrays. The worst of the arrays considered had 38 elements with negative radiation resistances, nearly half of the entire array. As was expected, the bad cases occurred mostly for $X^I/X_{11}=-1$ and -2, and more often for the small ka than for the larger ka. For ka=0.5, negative radiation resistances occurred over a wider band of X^I/X_{11} at small steering angles than for large steering angles. However, for ka=1.5, the only occurrences of negative radiation resistances were at large steering angles. Looking at Table IV as a whole, negative radiation resistances occurred slightly more often at larger steering angles.

CONCLUSIONS

Cavitation limited power is maximum for broadside steering and $Z^I=0$. It grows worse as the steering angle increases. Velocity limited power is maximum for $Z^I=\infty$, and occurred at some optimum steering angle which was dependent upon the size of the array, with the larger arrays having a greater optimum steering angle. Negative radiation resistances occurred slightly more often for larger steering angles; and for ka=1.5, they only occurred for large steering angles.

David T. Porter

David T. Porter
Mathematician

REFERENCES

(a) D. T. Porter, Effect of Thevenin Equivalent Internal Impedance on Velocity Control, etc., USL Report No. 648, 2 April 1965.

(b) D. T. Porter, Broadband Velocity Control, USL Tech Memo No. 960-47-65, 30 June 1965.

(c) C. H. Sherman, "Effect of the Nearfield on the Cavitation Limit of Transducers," Journal of the Acoustical Society of America, Vol. 35, No. 9, September, 1963, p. 1409.

(d) N. T. Chin, Radiation Resistance and Cavitation Factor of Rectangular Arrays with Beam Steering, USL Report No. 681, 8 November 1965.

TEST DATA RECORD
3ND-USNUSL-6

Sheet ___ of ___ Sheets

OBSERVER	DATE	BUSHIPS PROBLEM NO.

LAB JOB ORDER NO

TABLE II

EXPLANATION OF TEST

AVERAGE RADIATION RESISTANCES $R/\rho c A$

FOR 80 ELEMENT STEERED ARRAYS

	1 ka	2 X_I/X_{II}	3	4 BROADSIDE $\theta_{st} = 0°$	5 15°	6 30°	7 45°	8 60°	9 75°	10 ENDFIRE 90°	11
1	0.5	EQUAL VELOCITY ∞		.776	.776	.822	1.042	.990	.848	.785	
2		+1		.774	.787	.864	1.032	1.221	1.132	1.970	
3		0		.752	.772	.852	1.038	1.312	1.207	.945	
4		-1		.347	.070	.300	.178	.737	.120	-.049	
5		-2		.637	.822	.418	.242	.293	.273	.264	
6		-3		.769	1.030	.831	.690	.645	.567	.545	
7		-5		.746	.701	.927	1.110	.809	.664	.621	
8	1.0	EQUAL VELOCITY ∞		.789	.807	.864	.981	1.252	1.110	.975	
9		+1		.791	.813	.864	.982	1.269	1.468	1.273	
10		0		.789	.813	.866	.984	1.302	1.718	1.303	
11		-1		.650	.294	.263	.075	.051	.016	.068	
12		-2		.777	.819	.702	.632	.327	.497	.430	
13		-3		.767	.811	.826	1.010	1.223	.818	.700	
14		-5		.784	.802	.870	.970	1.322	.952	.823	
15	1.5	EQUAL VELOCITY ∞		.724	.801	.839	.813	1.104	1.165	1.161	
16		+1		.723	.812	.840	.818	1.111	1.279	1.213	
17		0		.728	.813	.848	.823	1.155	1.336	1.200	
18		-1		.734	.867	.857	.826	1.147	1.501	1.560	
19		-2		.728	.802	.852	1.013	.918	.188	.379	
20		-3		.724	.806	.850	.875	1.363	1.360	1.284	
21		-5		.723	.804	.849	.838	1.228	1.241	1.194	

3ND-PPPO-(1532)

TEST DATA RECORD
3ND-USNUSL-6

Sheet ___ of ___ Sheets

OBSERVER	DATE	BUSHIPS PROBLEM NO.
LAB JOB ORDER NO		

TABLE III

EXPLANATION OF TEST: AVERAGE RADIATION REACTANCES $X/\rho c A$ FOR 80 ELEMENT STEERED ARRAYS

	1 ka	2 X^I/X_{II}	3	4 BROADSIDE $\theta_{st}=0°$	5 15°	6 30°	7 45°	8 60°	9 75°	10 ENDFIRE 90°	11
1	0.5	EQUAL VELOCITY ∞		.166	152	.176	.397	.692	.863	908	
2	↓	+1		.153	159	186	.296	.618	1.089	1.237	
3		0		.133	.145	.172	266	.614	1267	1443	
4		−1		.194	450	338	375	.597	.444	455	
5		−2		.683	.485	633	.627	826	.803	.791	
6		−3		268	870	.323	1.061	892	.822	.793	
7	↓	−5		184	.195	−.027	.619	816	.856	.860	
8	1.0	EQUAL VELOCITY ∞		.123	.132	.156	.200	.555	1.020	1.149	
9	↓	+1		.124	128	154	211	.412	1.038	1.417	
10		0		135	137	160	.221	.364	1.174	1749	
11		−1		.211	.242	.516	.664	.485	.593	.608	
12		−2		220	.211	.216	.543	923	1.167	1106	
13		−3		.139	164	104	212	.626	1.107	1.083	
14	↓	−5		.122	145	138	.200	.678	1.076	1.116	
15	1.5	EQUAL VELOCITY ∞		.209	149	.179	345	680	1.492	1.714	
16	↓	+1		.205	.145	166	329	.534	1.356	1.681	
17		0		.202	.153	.164	328	.494	1.361	1.674	
18		−1		.209	155	.174	.344	.535	1.088	1.553	
19		−2		.215	.152	.173	.236	.597	1.574	1.359	
20		−3		.213	.151	174	340	638	1.598	1.729	
21	↓	−5		.210	.155	.183	363	.766	1.633	1.773	

(Over)

TEST DATA RECORD
3ND-USNUSL-6

Sheet ___ of ___ Sheets

OBSERVER	DATE	BUSHIPS PROBLEM NO.

LAB JOB ORDER NO

TABLE IV

EXPLANATION OF TEST

NUMBER OF ELEMENTS HAVING NEGATIVE RADIATION RESISTANCES IN 80 ELEMENT STEERED ARRAYS.

	1 ka	2 $\frac{X^E}{X_i}$	3	4 $\Theta =$ (STEERING ANGLE) 0°	5 15°	6 30°	7 45°	8 60°	9 75°	10 90°	11
1	0.5	1		0	0	0	0	0	0	0	
2		0		0	0	0	0	0	0	0	
3		-1		20	24	14	24	28	38	38	
4		-2		16	10	12	22	16	8	8	
5		-3		8	6	8	8	0	0	0	
6		-5		4	4	0	0	0	0	0	
7											
8	1.0	1		0	0	0	0	0	0	0	
9		0		0	0	0	0	0	0	0	
10		-1		4	16	16	24	28	32	34	
11		-2		4	4	10	10	12	6	4	
12		-3		0	2	2	0	2	0	0	
13		-5		0	0	0	0	0	0	0	
14											
15	15	1		0	0	0	0	0	0	0	
16		0		0	0	0	0	0	0	0	
17		-1		0	0	0	0	0	0	0	
18		-2		0	0	0	2	8	12	4	
19		-3		0	0	0	0	0	0	0	
20		-5		0	0	0	0	0	0	0	
21	NOTE: NEGATIVE RADIATION RESISTANCES DID NOT OCCUR FOR EQUAL VELOCITY CASES										

(Over)

COLUMBIA UNIVERSITY
HUDSON LABORATORIES
CONTRACT Nonr-266(84)

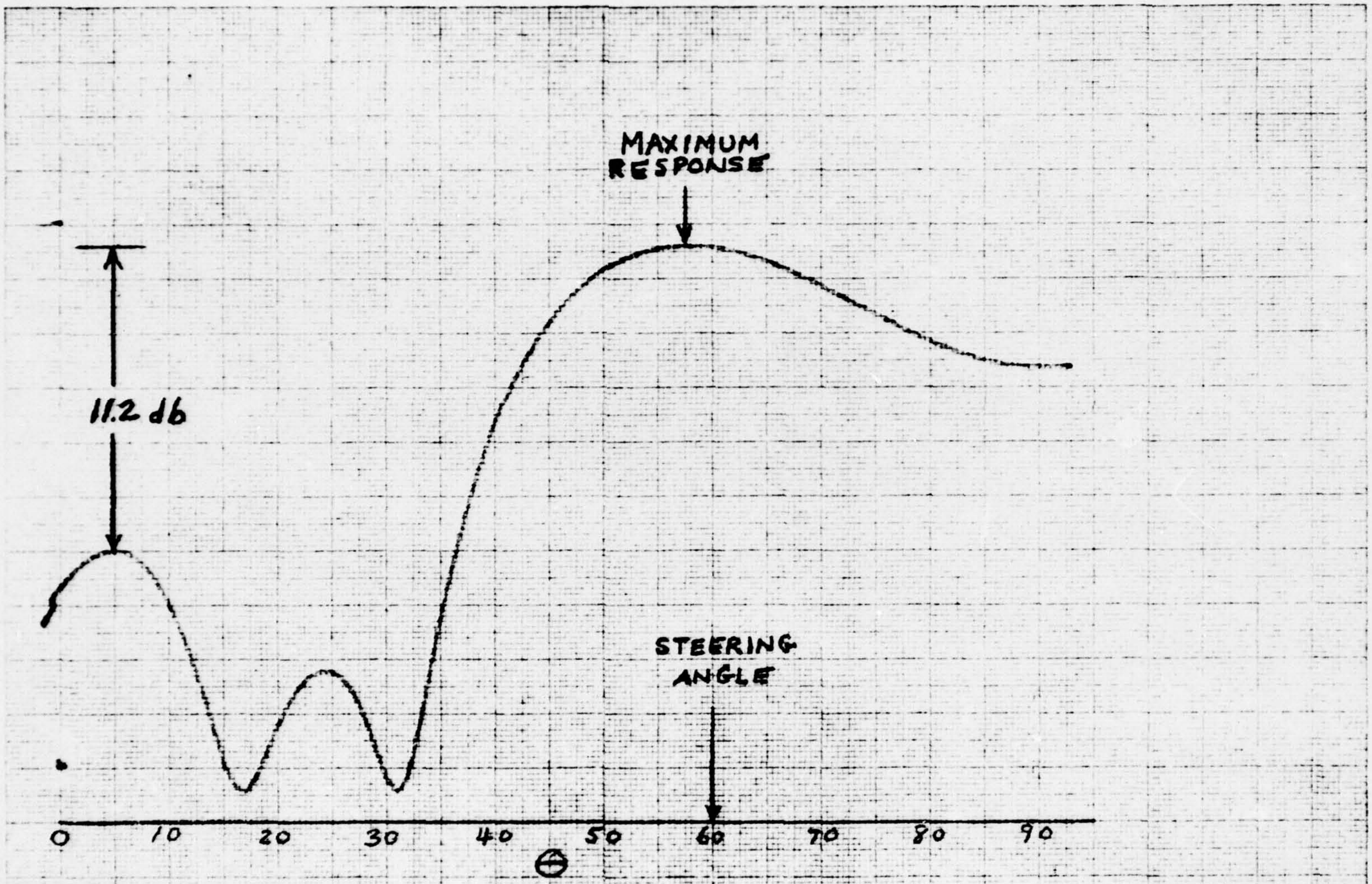

FIGURE 2
BEAM PATTERN FOR AN 80 ELEMENT ARRAY
$ka = 1.0,\ X^{\epsilon} = -X_{u},\ \Theta_{st} = 60°$

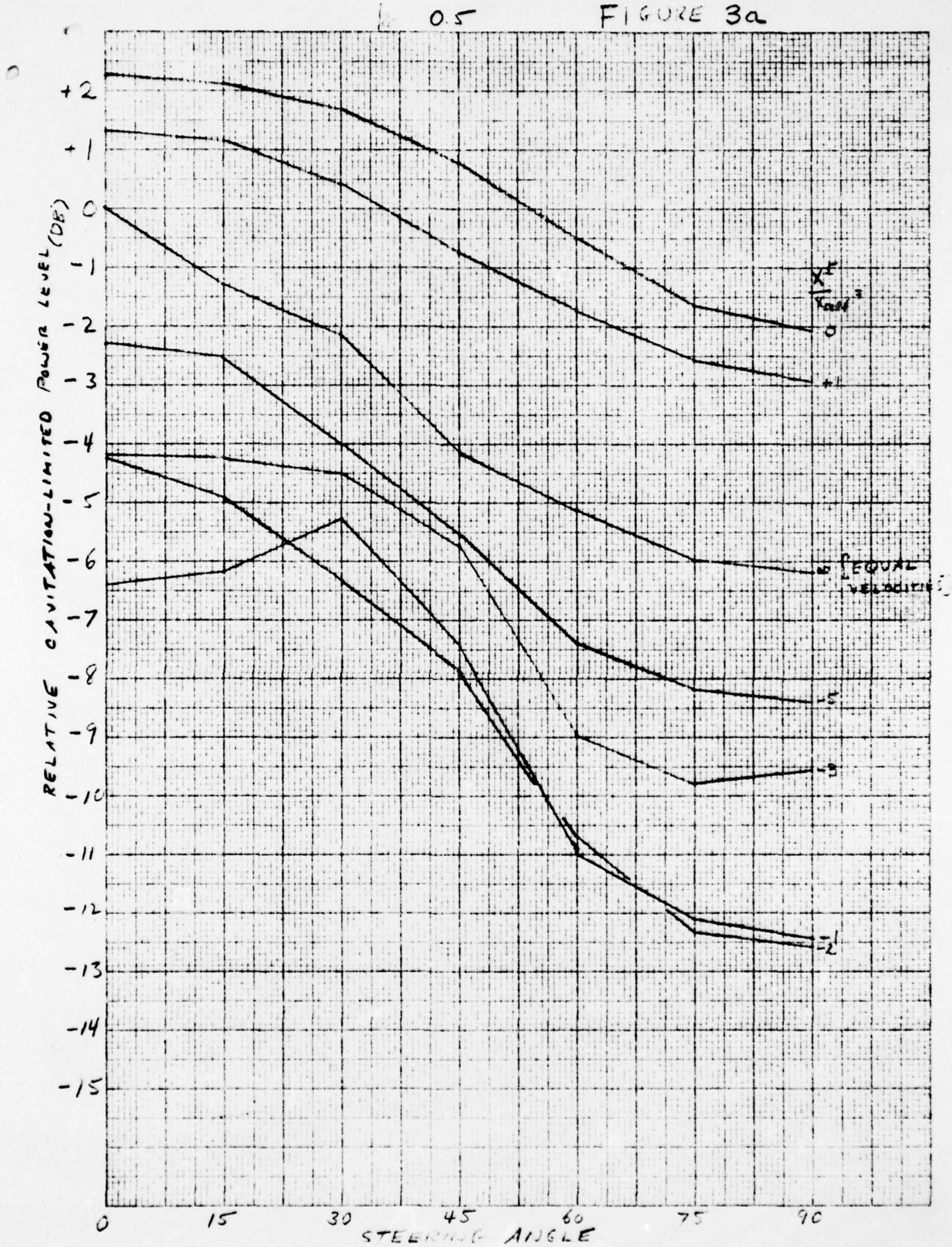

FIGURE 3a
0.5
+2
+1
0
-1
-2
-3
-4
-5
-6
-7
-8
-9
-10
-11
-12
-13
-14
-15
RELATIVE CAVITATION-LIMITED POWER LEVEL (DB)
0
15
30
45
60
75
90
STEERING ANGLE
0
+1
∞ EQUAL VELOCITIES
-5
-3
-1
-2

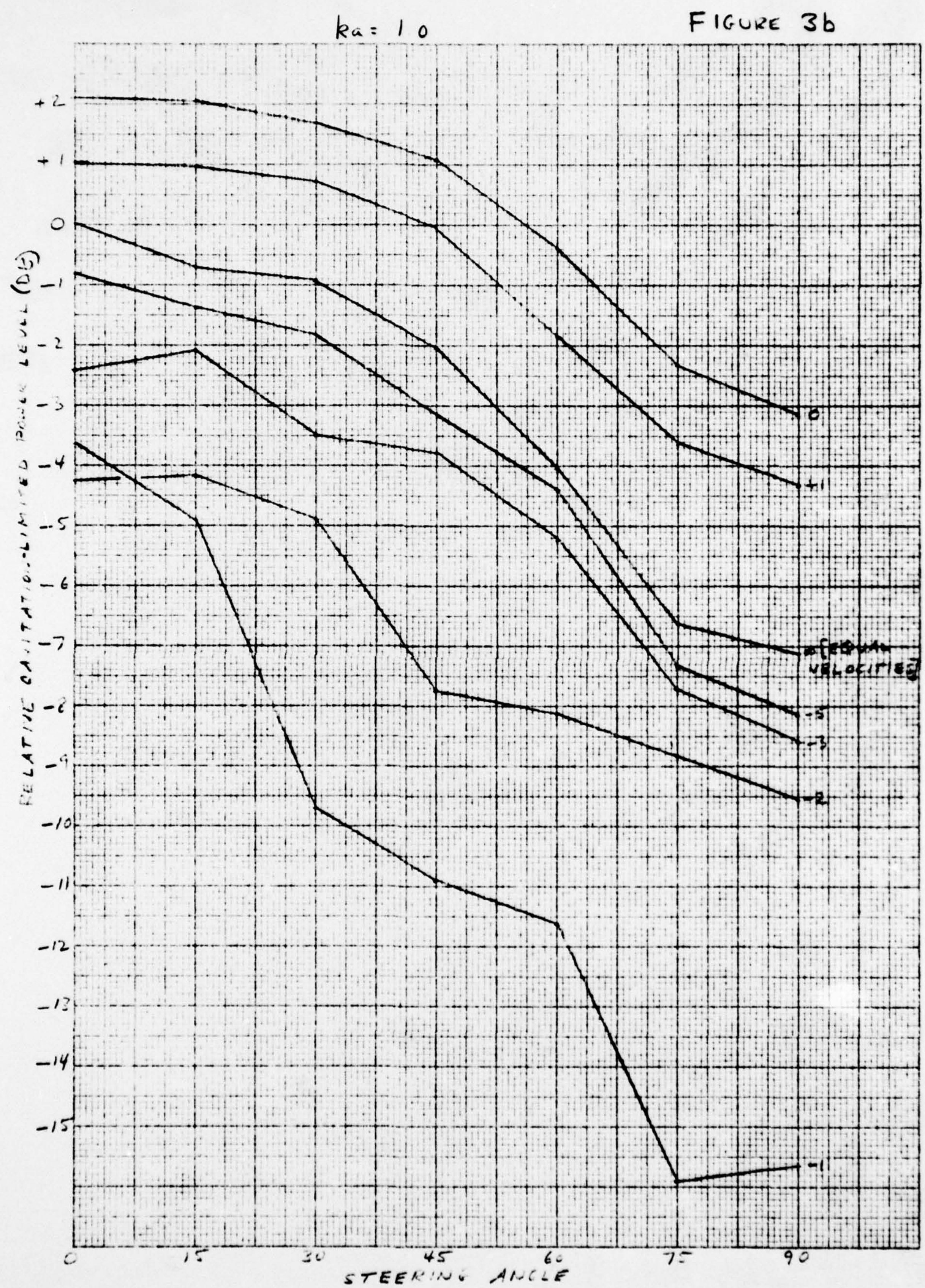
ka = 10
FIGURE 3b
RELATIVE CAVITATION-LIMITED POWER LEVEL (DB)
+2
+1
0
-1
-2
-3
-4
-5
-6
-7
-8
-9
-10
-11
-12
-13
-14
-15
0
15
30
45
60
75
90
STEERING ANGLE
+1
-5
-3
-2
-1

ka= 1.5

FIGURE 3a

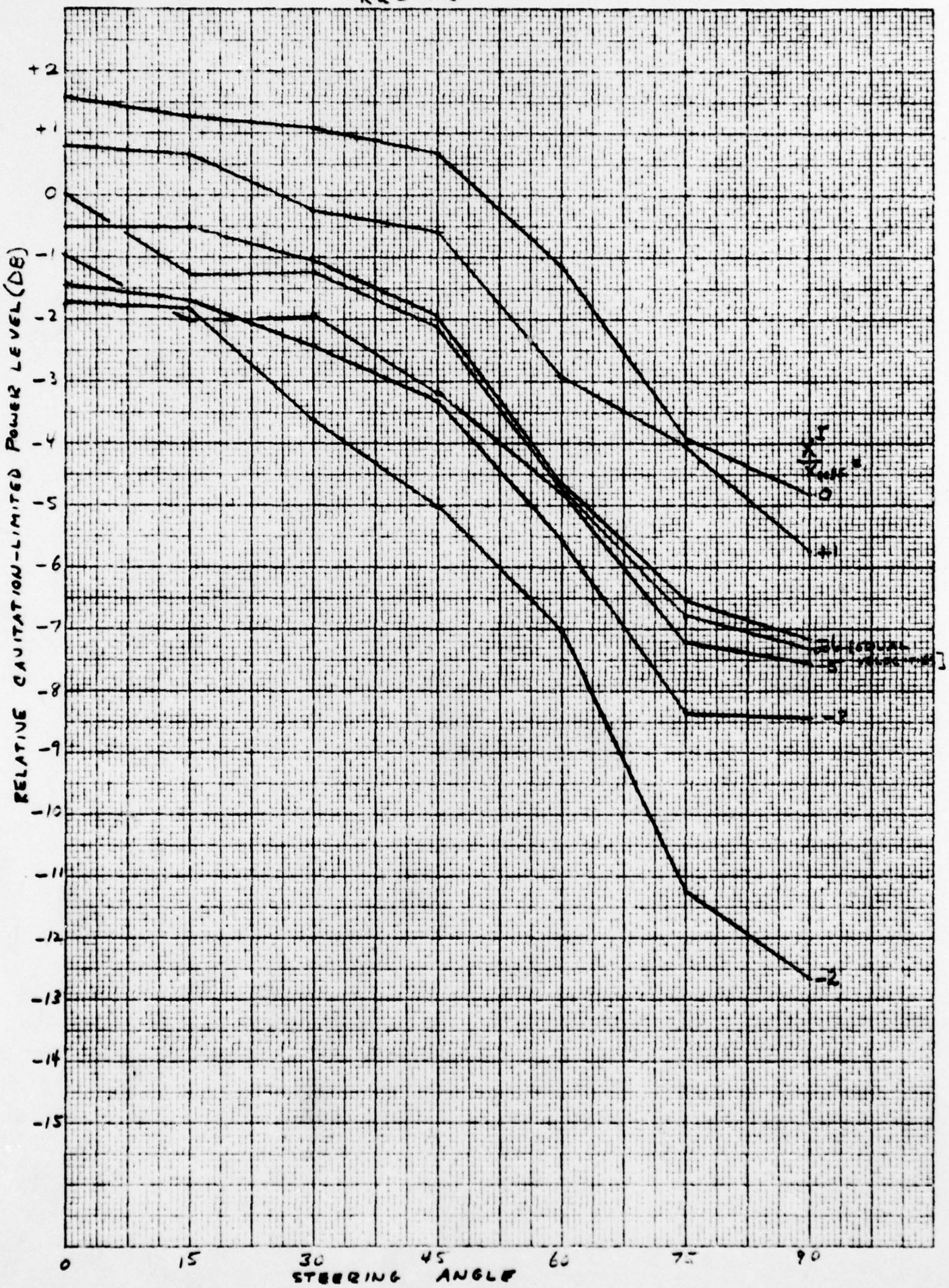

FIGURE 4a

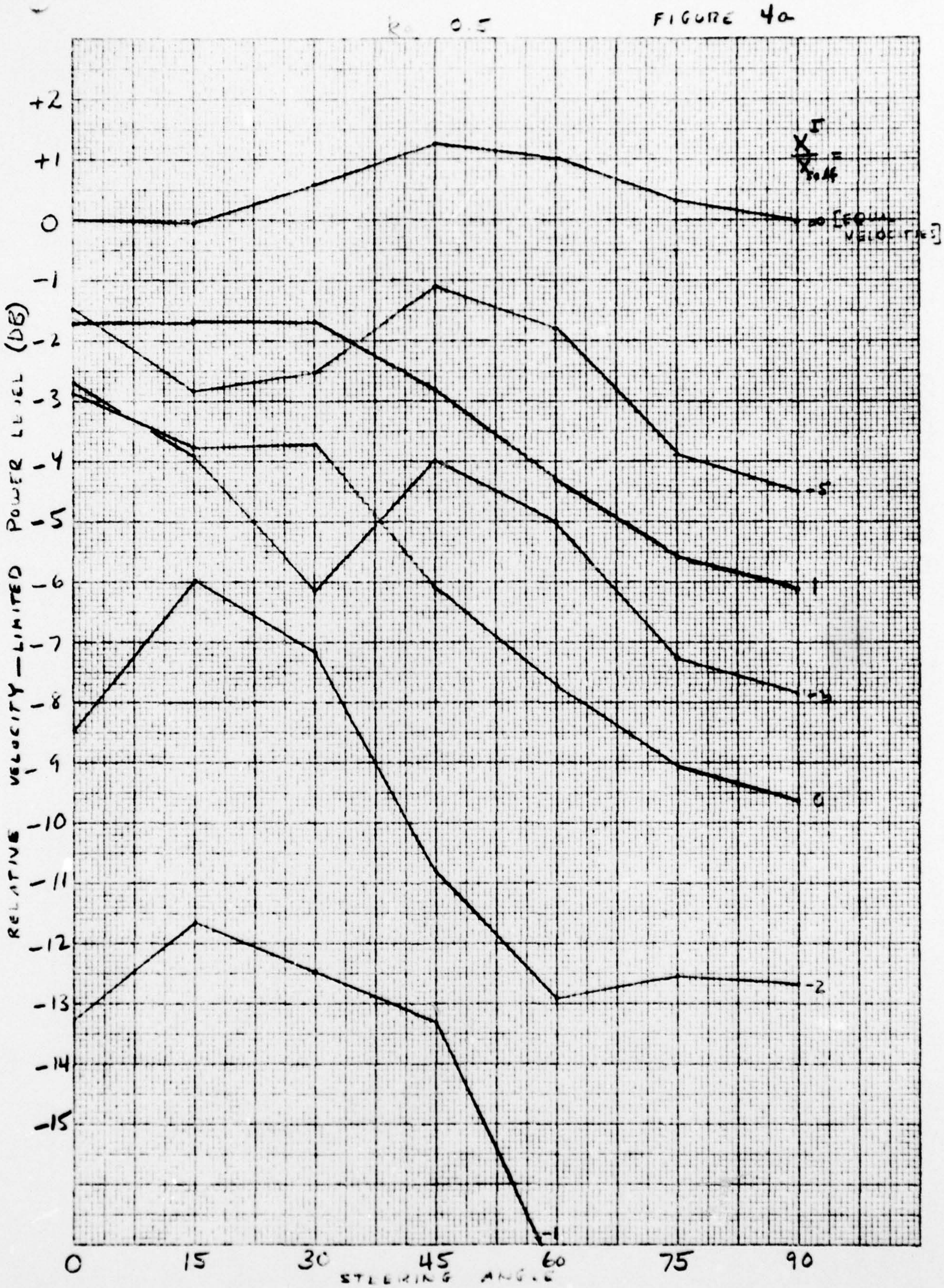

RELATIVE VELOCITY—LIMITED POWER LEVEL (DB)
STEERING ANGLE
+2
+1
0
-1
-2
-3
-4
-5
-6
-7
-8
-9
-10
-11
-12
-13
-14
-15
0
15
30
45
60
75
90
∞ [EQUAL VELOCITIES]
-.5
1
-.2
-2
-1

FIGURE 46

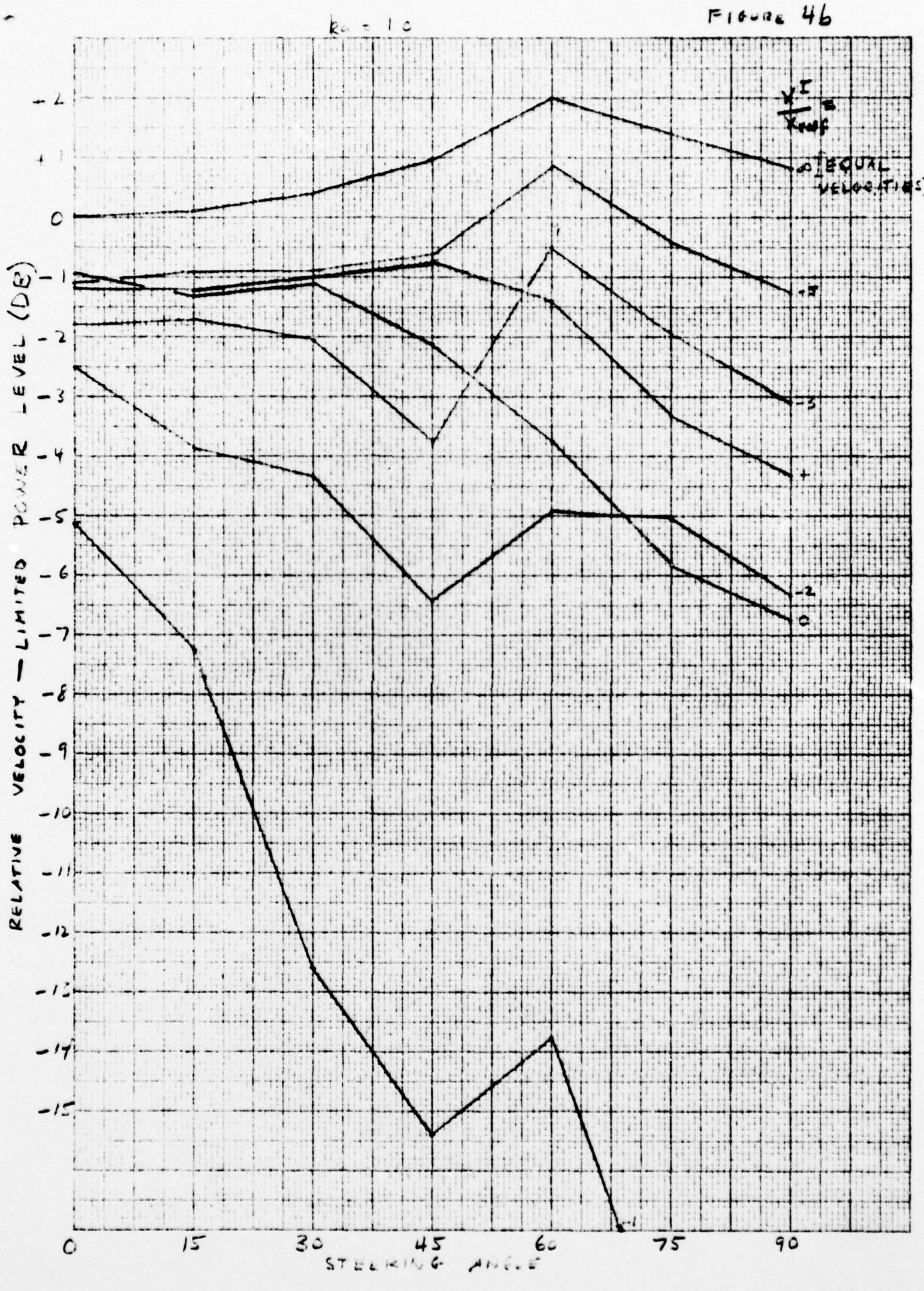
ka = 10
RELATIVE VELOCITY — LIMITED POWER LEVEL (DB)
STEERING ANGLE
+2
+1
0
-1
-2
-3
-4
-5
-6
-7
-8
-9
-10
-11
-12
-13
-14
-15
0
15
30
45
60
75
90
∞ [EQUAL VELOCITIES]
-2
0

FIGURE 4C

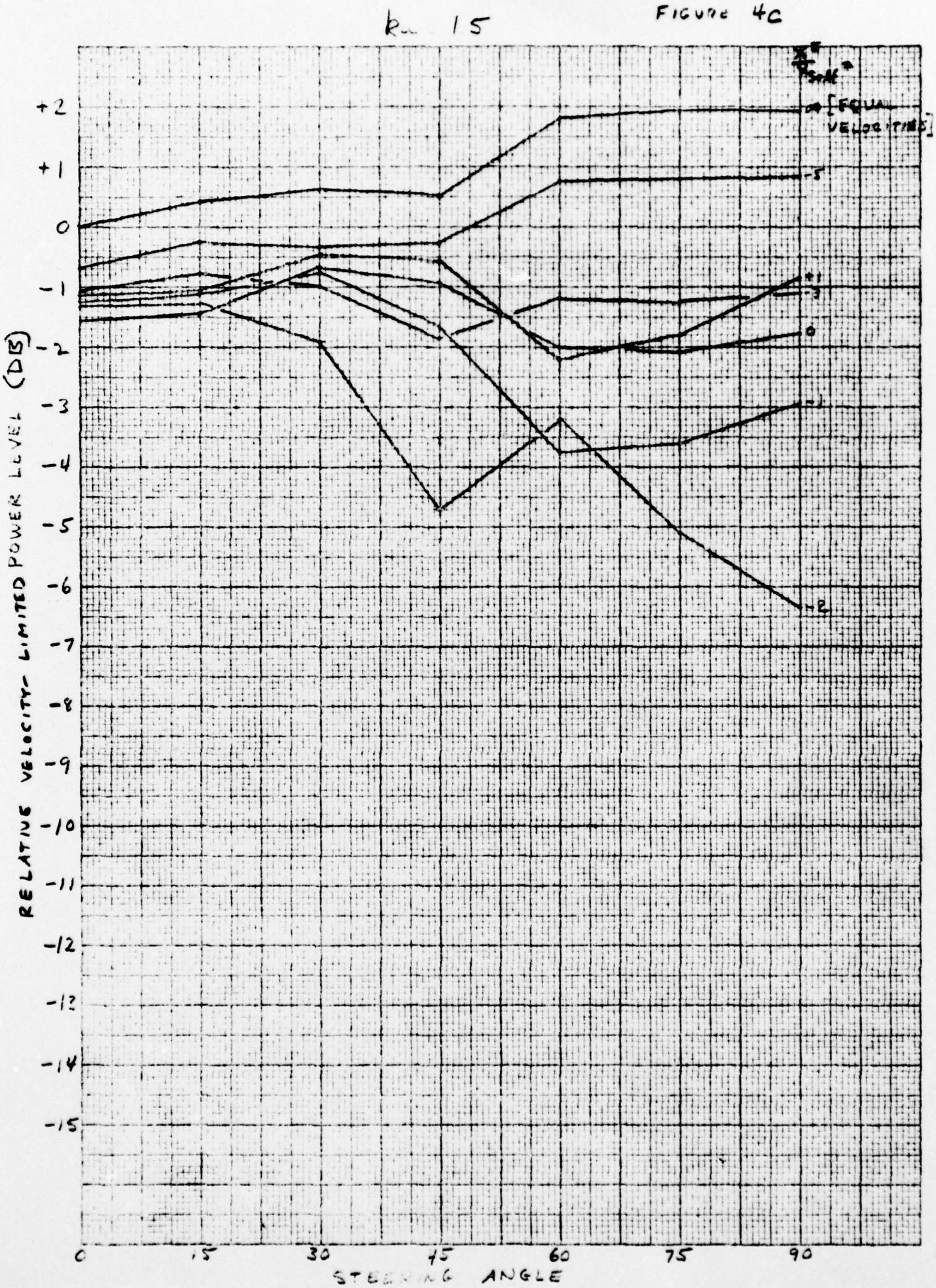

15
RELATIVE VELOCITY-LIMITED POWER LEVEL (DB)
+2
+1
0
-1
-2
-3
-4
-5
-6
-7
-8
-9
-10
-11
-12
-13
-14
-15
0
15
30
45
60
75
90
ANGLE
[EQUAL VELOCITIES]
-5
+1
-3
0
-1
-2